

Numerical Convection of Viscoelastic Magnetic Flows Past a Backward Facing Step Channel

Cheng-Hsing Hsu, Kuang-Yung Kung, Shu-Yu Hu
kykoung@gmail.com

Abstract—Numerical simulation presented viscoelastic magnetic flow past a backward facing step channel. The parameters of Richardson Number, Reynolds Number, elastic coefficient, buoyancy effects and magnetic field parameters were studied. The larger buoyancy effect was along with a larger Richardson Number. Transient coexistence of multiple second recirculation zone appear in downstream. The four symmetry vortexes appeared on the upper and lower plate. The oscillation phenomena were similar to Karman vortex. Under the same Richardson Number, Reynolds Number, and the elastic coefficient, the higher the magnetic field parameters resulted to the shorter length of the main and second recirculation zone.

Keywords—Buoyancy effect, Elastic coefficient, Magnetic field parameter, Viscoelastic magnetic fluid.

I. INTRODUCTION

In recent years, due to the rapid development of electronics industry, the electronics industry output has become a staple of many. Visco-elastic magnetic fluid applications in the industrial areas draw much attention, such as Non-Newtonian fluid transport and heat transfer phenomena. The visco-elastic magnetic fluid and Newtonian fluid flow characteristics have great differences. Scholars had established the theory of magnetic fluid visco-elastic foundation and processing mode, and analysed the visco-elastic magnetic fluid and The Newtonian fluid. The electromagnetic interference affected the working environment and quality of the products.

After the flow field of the study to the backward facing step on the Newtonian fluid, over the years has been taken seriously. Because the flow field includes the phenomenon of flow separation and reattachment, the flow characteristics can be demonstrated very clearly low, and furthermore because of its simple geometry and easy analysis. However, in engineering applications, such as positive and negative electrode membrane fuel cell reaction between hydrogen and oxygen can also be used to step upon the downstream vortex flow field to promote the hydrogen produced by reaction to an adequate response, and then to a higher efficiency of chemical reactions purpose.

Integral equation was using the second order model and the Maxwell model. Second mode in which all the higher order nonlinear terms to the stress tensor, that its behalf into the momentum equation. Such models are mainly used in small

magnetic visco-elastic fluid. The Maxwell model must be more than the introduction of a relaxation time, the stress tensor as independent variables, and this model is mainly used in large magnetic visco-elastic fluid.

The main purpose of this paper is to use numerical simulation to explore the magnetic field fixed at the high Richardson Number of cases. The second model visco-elastic magnetic fluid flow in the backward facing step is expected that the visco-elastic magnetic fluid in the post flow to the backward facing step to have a better understanding of the characteristics.

Backward step of the flow phenomenon has been valued by everyone. The flow fields in supersonic flow first by Hama experiment found that supersonic fluid flow through the backward facing step after the sharp corners produced by separation. The main reason for the Reynolds Number is small, the separation angle from near the concave production ladder. When the Reynolds Number is large, concave angle generated in addition to separation, will be followed by another in the convex corner separation near the production area.

In 1975 Honji [1] observed by the experiments re-attachment length increases with time to lower growth and time is about a linear relationship. Armaly et [2] were also from the experimental and numerical methods that, when the Reynolds Number is greater than 420, the order form in a relatively flat area above the board has time back production. When the Reynolds Number increased to 980, the lower plate near the downstream of the primary recirculation zone will also produce another. The numerical results are compared with the experimental data; the Reynolds Number less than four hundreds, both errors is really small. But more than this range, three-dimensional effect by enhancing the flow field, resulting in two-dimensional numerical simulation lead to considerable error.

Durst and Pereia [3] After using the TEACH code on the backward facing step to do transient flow analysis, when the Reynolds Number equal to ten, divided off from the concave angle to start production, increase over time along the vertical ladder climbing rose. In the Reynolds Number is equal to 368, and then the concave corner and convex corner vortex near the emergence of an independent, gradually increasing over time merge. And there have been times back on the flat area, but stable before has disappeared.

There are a number of other studies, such as Sparrow and Chuck [4] through personal computers, calculation of steady forced convection flow, analysis of step height and Reynolds

Number on the reattachment length and the impact and return to the region of thermal convection effect. Chein [5] using stream function and vorticity equations for computing functions, with the continuous relaxation, the first order explicit upwind finite difference method and the circulation flow theory for transient analysis.

John and Leone [6] to finite element analysis of the backward facing step in steady mixed convection flow. In the ladder above the heating plate and found that the Richardson Number of logical investigation is equal to 9 or 16, the Reynolds Number is equal to 800, Prandtl Number is equal to 1, the ladder, there are three vortex downstream plate, heating two vortex appeared on board, paper, and to explore the effects of different export length. Lin and Armaly [7] The TEACH code analysis of the vertical pipe after the backward facing step steady mixed convection. Found that increased buoyancy will shorten the length of re-engagement, increase in the ladder flat concave corner recirculation zone times the range. When the buoyancy generated by increased starved flow, then the vertical ladder access point is located, their locations back to the highest point of heat transfer area in contact point further downstream. The size and Nusselt Number of local enhanced with the buoyancy of the gain in great, although the backward facing step with the analysis of flow field is highly valued, but most of Newtonian fluid as the main target.

For visco-elastic fluid flow field after the backward facing step is rarely discussed phenomenon. Only Kawabata et [8] The Maxwell model of steady-state flow phenomena found in the same Reynolds Number, visco-elastic fluid in the lower speed step slower than the Newtonian fluid. In recent years, the backward facing step after the special study areas Chan et [9] used the Improved Stochastic Separated Flow (ISSF) numerical simulation of gas - particle flow in the latter case the flow to the backward facing step. Found its way analysis of anisotropic particle flow disorder has a good effect. Piccolo et [10] used the numerical simulation analysis of the primary recirculation zone to the backward facing step and external fluid exchange between the disturbed stream function, the paper can be found to the convective flow downstream due to the interaction of disturbance associated with discontinuous shear surface caused by the periodic large-scale vortex in the backward facing step, the primary recirculation zone showed the coexistence of two-vortex phenomenon, and even the formation of the downstream area of a small time back. Currently used in the relevant experimental environment. Such as, the loop structure between the drainage of waste water pollution emissions.

Bassam A/K Abu-Hijleh [11] after the vertical backward facing step to the ladder below the material into the porous medium to study the effects of heat transfer. When the maximum Nusselt Number of local to 170% reduction in the Nusselt Number of total 16%. Kim and Baek [12] the backward facing step combination of radiation, convection, conduction, application of flow to the backward facing step, because the effects of radiation, let the temperature rise rapidly. Also, because adverse pressure gradient decreases, leading to longer

contact length will be reduced. Abu-Milaweh [13], and others use the Doppler and cold wire anemometer to do the vertical ladder of the disorder after the measurement of mixed convection experiment, found a small free stream will result in turbulence intensity decreases, while the convective line position, cross-section rate and temperature difference. The longer contact length with the lower heating plate, the heat transfer rate decreases.

The mutant form of the researchers in terms of elastic fluids, is a major problem, especially in corners of the deal more complex than the Newtonian fluid, it is often the determining factor in numerical convergence. In addition there are visco-elastic fluid heat transfer characteristics, the literature not many. Only early Vest and Arpac [14] Herbert [15] and mathematical analysis of the way of a visco-elastic fluid heated in the flat state of stability. Hsu and Chieng [16], Chen and Teng [17] while the second model of a visco-elastic fluid in a continuous moving plate and a wedge on the flow of heat transfer analysis. Hsu and Chou [18] The visco-elastic fluid flow in the backward facing step phenomena, compare different Reynolds Number and elasticity of the flow field development under the circumstances. Hsu et [19] also discussed the visco-elastic fluid in different Richardson Number, Reynolds Number and elastic modulus of the backward facing step field. In Richardson Number is defined as the buoyancy effect. When Richardson Number increases, the primary recirculation zone will increase, while the increase elasticity to reduce the scope. Thermal boundary layer flow field increases with time, gradually from the lower plate to the thickening of the internal flow field. When Richardson Number is equal to 1, elastic coefficient is equal to 0.001, and the Reynolds number of 50 and 75, the reattachment length of its overshoot phenomenon. This is no place Newtonian fluid flow characteristics. So, the Richardson Number of 1, elastic coefficient of 0.001, and the Reynolds Number 75, have a steady second recirculation zone exists.

Hsu and Kung [20] while further are adding the change of flow angle of the visco-elastic fluid on the backward facing step after the impact of transient mixed convection. Found that the reattachment length increases gradually as the angle increased to the maximum value and then decrease as the angle increases, the maximum angle in the flow channel 150 or 180 degrees. When the Reynolds Number increases, and the visco-elastic coefficient is small, there will be a larger reattachment length, and in this case, the flow angle near 180 degrees, and then attached to the length of the length of time different from the other angle would be more than the local Nusselt Number maximum value position.

In 1930 by the physicist Bitter and Hamos et for the first time to research the use of strong magnetic solution, using strong magnetic colloidal solution to observe the sector in the state of colloidal particles. At that time, however, will only focus on the colloidal particles are accumulated on magnetic area, the nature of magnetic wall, did not consider the strong magnetic colloidal stability in solution, Therefore the magnetic colloid was at that

time different the magnetic fluid which research at present. It means the magnetic fluid is may stabilize disperses in the middle of the solvent, by magnet attraction, but does not precipitate.

Wang [21] through theory and numerical analysis for the stable, non-compression transmission fluid MHD fully developed flow conditions, subject to a uniform transverse magnetic field of the vertical channels to consider the magnetic field, viscous dissipation, internal heat source and channel wall surface temperature. After the system of governing equations in dimensionless Office, the numerical solution using Runge-Kutta method was approximate solution and theoretical solution obtained by the introduction of perturbation series. Where perturbation parameters is $B\bar{r}G\bar{r}/Re = \varepsilon$. For the small perturbation parameters and the results very close to the numerical solutions, but with the perturbation parameter increases, the theory of approximation and numerical approximation of difference between the results obtained also increases.

Hong [22] used the numerical simulation of airflow in the clean room work flow through the machine, the resulting flow field and magnetic field changes. The use of third-order upwind finite volume method and second order central interpolation points to two-dimensional MHD equations demand, and in the continuity equation by adding artificial compression factor method. Including the use of high-order upwind finite volume techniques, in the viscous item by second order finite volume method is adopted. The adoption of the second-order central difference to calculates the magnetic field, because the magnetic field divergence conservation in magnetic field. Shows the magnetic field parameters were restrained for the eddy current; magnetic field strength in addition to boundary layer separation can prevent the production of things, when the magnetic field strength in the boundary layer was large enough, the flow lines become narrower and with a little acceleration produced.

Weng [23] by numerical simulation of non-Newtonian fluids in non-uniform magnetic field plate flow stream flow fields, and then explore the related flow field. That factor in the effect of non-Newtonian acceleration and angular velocity of the benefit changes, the magnetic field strength will decrease with the increase. Also, get the best flow rate and the best resistance of the magnetic fluid flow characteristics. When the largest non-Newtonian conditions, and can find the best ratio of relaxation times $\Gamma = 0.1$.

According to the above literature review, the backward facing step can be seen in the post within the complex equation of the visco-elastic composition of the transient mixed convection MHD problem, not only in industry is useful and, in the academic discussion is also very important, This paper also Richardson Number, the buoyancy effect and magnetic effect of mutual relations between the flow field after the phenomenon to the backward facing step.

In this paper, the second mode visco-elastic magnetic fluid flow in the backward facing step by the transient analysis, numerical simulation analysis of the main mining method.

Dealing with highly nonlinear equations for the governing equations, the numerical processing procedure must be linear and constant iteration by computing and convergence results obtained. Related numerical iterative method is Line Gauss-Seidel Method and interaction with the application of scanning method. Because of nonlinear equations in linear processing into the iterative calculation may cause numerical divergence, so also in the vorticity stream function and adding under-relaxation and over-relaxation method, in order to avoid this phenomenon.

Problem Formulations

Magnetic Fluid is the magnetic ultrafine particles will surface treatment, stable dispersion in water or organic liquid media content such as the suspension liquid by magnetic or gravity field of the magnetic particles will not be under produce condensation and precipitation. Therefore, the size of ferromagnetic particles cannot be too large, or because of their gravity and precipitation phenomena. It's very small due to the strong magnetic particles, so the appearance is no longer with the naked eye to distinguish the different fluids and liquids, the solution may be regarded as a mixture.

Although the magnetic fluid is a liquid, the magnet will be attracted to a magnetic field gradient for magnetic fluid placed under the strong magnetic ultrafine particles in the magnetic field strength of the party by the magnetic, strong magnetic ultrafine particles collide with solvent molecules irregular. Imposed on the strong magnetic ultrafine particles reached the bulk solution, as apparent as the entire solution on the role of magnetic force are subject to being attracted to magnetic material, so if a liquid fluid in appearance, but with iron, nickel, can also be a magnet to attract. General magnetic fluid process can be divided into two stages, first into ultrafine particles of high magnetic material or processing ultrafine particles shape process, what is to prevent the aggregation of high magnetic ultrafine particles to the surfactant which surrounds the magnetic ultrafine particles dispersed in the liquid-based process.

Description and Assumption

This paper studies the transient visco-elastic MHD mixed convection in the high number of under Richardson stepped in after the characteristics of flows. Analysis of flow characteristics of fluid flow include transient and steady-state phenomenon.

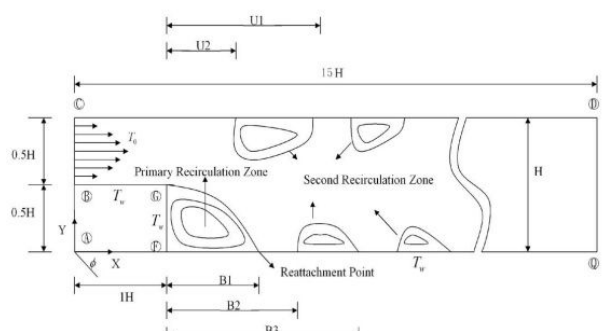


Fig.1 flow diagram of the geometric model.

Fig.1 show step height $S = 0.5$, step width $d = 1.0$, flow height $H = 1.0$, the total flow length $L = 15H$, the assumption that the total length of flow is determined by the width ladder, but will depend on the length of follow-up notes and re-further discussion. Solid boundaries are assumed to flow to no-slip condition. For ease of discussion, the paper plate under the definition of ladder near the recirculation zone generated by the premises known as the primary recirculation zone, the back plate area and the second occurred under the flat area called the meeting back to back district.

Analysis of mixed convection flow, the more complex governing equations, buoyancy assuming of the Boussinesq model remains a simplified model.

Geometric model of the above plus the following assumptions as the basis of this study:

- 1) Consider the two-dimensional laminar flow, incompressible magnetic fluid.
- 2) Visco-elastic fluid is secondary magnetic fluid.
- 3) Fluid density and other physical properties are constants.
- 4) Ladder entrance at the upstream flow state for the fully-developed flow.
- 5) Exporting state in the downstream flow along the flow direction parameter change was zero for Newman boundary conditions.
- 6) Energy equation is not considered magnetic dissipation of the effect of viscosity.
- 7) Magnetic field intensity is constant.

A. Governing Equations

In the static magnetic field, magnetic flux density B required to take into account the two basic assumptions:

$$\nabla \cdot B = 0 \quad (1)$$

$$\nabla \times B = \mu_0 J \quad (2)$$

Simultaneously wants satisfies the time-variable electric charge under condition, then Maxwell Equation the general form is:

$$\nabla \cdot B = 0 \quad (3)$$

$$\nabla \times \bar{E} = -\frac{\partial B}{\partial t} \quad (4)$$

$$\nabla \times h = J + \frac{\partial D}{\partial t} \quad (5)$$

$$\nabla \cdot D = q \quad (6)$$

where $h (\equiv B/\mu_0)$ is magnetic field intensity, B is magnetic flux density, D is electric flux density, $\bar{E} (\equiv D/\epsilon_0)$ is electric field, $J (\equiv \sigma \bar{E})$ is conduction current density, σ is electric conductivity.

Where $\mu_0 (\equiv 4\pi \times 10^{-7} \text{ Henrys/m})$, $\epsilon_0 (\equiv 8.85 \times 10^{-12} \text{ F/m})$, equations (5) and (6) can be written as following.

$$\frac{\partial q}{\partial t} + \nabla \cdot J = 0 \quad (7)$$

Neglects the displacement current by the foundation electric

charge theory, Maxwell equations can be simplified:

$$\nabla \cdot B = 0$$

$$\nabla \times \bar{E} = -\frac{\partial B}{\partial t} \quad (8)$$

$$\nabla \times h = J$$

The $h (\equiv B/\mu_0)$ into (8), which can be rewritten as:

$$\nabla \times B = \mu_0 J \quad (9)$$

If the same space with electric and magnetic fields exist, then the point in which the forces on the charge is the sum of static electricity and magnetism, known as the electromagnetic force or the Lorentz force is called Ohm's law.

$$J = \sigma(\bar{E} + u \times B) \quad (10)$$

That considered the main magnetic field volume B , by Ohm's law to take every type of curl, then Faraday's law and Ampere's law into the available magnetic induction equation.

$$\frac{\partial B}{\partial t} = \nabla \times (u \times B) + \frac{1}{\mu_0 \sigma} \nabla^2 B \quad (11)$$

Momentum equation in the external force, it is itself composed of gravity and the Laplace force.

$$\rho f = \rho g + J \times B \quad (12)$$

Basically a visco-elastic magnetic fluid viscosity, elasticity and magnetic properties of three, but only have the sticky nature of the Newtonian fluid, so we need to re-derive the visco-elastic constitutive equation of magnetic fluid, so that the composition of visco-elastic fluids with viscous equations , three kinds of elastic and magnetic properties.

Elastic properties of an object are deformed by the force of its own to restore the shape of a memory feature. When the analysis of uniform incompressible visco-elastic magnetic fluid through the second after the step flow field, we describe the stress of such fluid flow by Rivlin and Ericksen form [24] model. Stress tensor scales as:

$$\mathbf{T} = -(p + \frac{1}{2} h \times (\nabla \times B)) \mathbf{I} + \mu \mathbf{A}_1 + \alpha_1 \mathbf{A}_2 + \alpha_2 \mathbf{A}_1^2 \quad (13)$$

$$\mathbf{A}_1 = \text{grad } \mathbf{V} + (\text{grad } \mathbf{V})^T \quad (14)$$

$$\mathbf{A}_2 = \frac{d}{dt} \mathbf{A}_1 + \mathbf{A}_1 (\text{grad } \mathbf{V}) + (\text{grad } \mathbf{V})^T \mathbf{A}_1 \quad (15)$$

Where \mathbf{V} is velocity, d/dt is material time derivative. Rajagopal [25] such as the approach, we can equation (13) into the momentum equation is

$$\rho \frac{d}{dt} \mathbf{V} = \text{div} \mathbf{T} + \rho \vec{b} \quad (16)$$

And by assuming a two-dimensional incompressible laminar flow, so $\text{div} \mathbf{V} = 0$. The body force $\vec{b} = \nabla \phi$ is the conservative force field, and define it is

$$\mathbf{P} = p - \alpha_1 \mathbf{V} \cdot \nabla^2 \mathbf{V} - (2\alpha_1 + \alpha_2) |\mathbf{A}_1|^2 + \frac{1}{2} \rho |\mathbf{V}|^2 + \rho \phi \quad (17)$$

In addition, the Rajagopal and Fosdick [27] show the results of the thermodynamic derivation.

$$\mu \geq 0, \alpha_1 \geq 0, \alpha_1 + \alpha_2 = 0 \quad (18)$$

We can replace α_2 with α_1 . And consider the fluid in the horizontal direction and vertical direction by the buoyancy of the size of the respective B_x and B_y .

$$B_x = g\beta(T_w - T_0)\sin\phi \quad (19)$$

$$B_y = g\beta(T_w - T_0)\cos\phi \quad (20)$$

Where ϕ is the angle between flow channel axis and the directions of gravity.

Finally available related to the governing equations for the second order visco-elastic fluids are:

Continuity equation:

$$\frac{\partial u}{\partial x} + \frac{\partial v}{\partial y} = 0 \quad (21)$$

Momentum equation:

$$\begin{aligned} \frac{\partial u}{\partial t} + u \frac{\partial u}{\partial x} + v \frac{\partial u}{\partial y} &= \\ -\frac{1}{\rho} \frac{\partial p}{\partial x} + \frac{\mu}{\rho} \left(\frac{\partial^2 u}{\partial x^2} + \frac{\partial^2 u}{\partial y^2} \right) & \\ + \frac{\alpha_1}{\rho} \left[\left(\frac{\partial^3 u}{\partial x^2 \partial t} + \frac{\partial^3 u}{\partial y^2 \partial t} \right) + 2 \frac{\partial^2}{\partial x^2} \left(u \frac{\partial u}{\partial x} + v \frac{\partial u}{\partial y} \right) \right. & \quad (22) \\ + 4 \left(\frac{\partial u}{\partial x} \frac{\partial^2 u}{\partial x^2} + \frac{\partial v}{\partial x} \frac{\partial^2 v}{\partial x^2} \right) + \frac{\partial^2}{\partial x \partial y} \left(u \frac{\partial v}{\partial x} + v \frac{\partial v}{\partial y} \right) & \\ + \frac{\partial^2}{\partial y^2} \left(u \frac{\partial u}{\partial x} + v \frac{\partial u}{\partial y} \right) + 2 \frac{\partial}{\partial y} \left(\frac{\partial u}{\partial x} \frac{\partial u}{\partial y} + \frac{\partial v}{\partial x} \frac{\partial v}{\partial y} \right) & \\ + g\beta(T_w - T_0) \sin\phi - \frac{\sigma}{\rho} \bar{b}(\bar{b}u - \bar{a}v) & \end{aligned}$$

$$\begin{aligned} \frac{\partial v}{\partial t} + u \frac{\partial v}{\partial x} + v \frac{\partial v}{\partial y} &= \\ -\frac{1}{\rho} \frac{\partial p}{\partial y} + \frac{\mu}{\rho} \left(\frac{\partial^2 v}{\partial x^2} + \frac{\partial^2 v}{\partial y^2} \right) & \\ + \frac{\alpha_1}{\rho} \left[\left(\frac{\partial^3 v}{\partial x^2 \partial t} + \frac{\partial^3 v}{\partial y^2 \partial t} \right) + 2 \frac{\partial^2}{\partial y^2} \left(u \frac{\partial v}{\partial x} + v \frac{\partial v}{\partial y} \right) \right. & \quad (23) \\ + 4 \left(\frac{\partial u}{\partial y} \frac{\partial^2 v}{\partial y^2} + \frac{\partial v}{\partial y} \frac{\partial^2 v}{\partial y^2} \right) + \frac{\partial^2}{\partial x \partial y} \left(u \frac{\partial u}{\partial x} + v \frac{\partial u}{\partial y} \right) & \\ + \frac{\partial^2}{\partial x^2} \left(u \frac{\partial v}{\partial x} + v \frac{\partial v}{\partial y} \right) + 2 \frac{\partial}{\partial x} \left(\frac{\partial u}{\partial x} \frac{\partial u}{\partial y} + \frac{\partial v}{\partial x} \frac{\partial v}{\partial y} \right) & \\ + g\beta(T_w - T_0) \cos\phi - \frac{\sigma}{\rho} \bar{a}(\bar{a}v - \bar{b}u) & \end{aligned}$$

Energy equation:

$$\frac{\partial T}{\partial t} + u \frac{\partial T}{\partial x} + v \frac{\partial T}{\partial y} = \alpha \left(\frac{\partial^2 T}{\partial x^2} + \frac{\partial^2 T}{\partial y^2} \right) \quad (24)$$

Where ρ is the density, \bar{a}, \bar{b} respectively x, y direction of the magnetic field, μ is dynamic viscosity coefficient, and the constants α are the thermal diffusion coefficient. α_1 is related with the fluid elasticity coefficient, the value of the fluid nature of the decision.

B. Dimensionless Parameter

The governing equations introduce the dimensionless parameters. The relevant dimensionless parameter is defined as:

$$X = \frac{x}{H}, Y = \frac{y}{H}, a = \frac{\bar{a}}{B}, b = \frac{\bar{b}}{B} \quad (25)$$

$$U = \frac{u}{U_0}, V = \frac{v}{U_0} \quad (26)$$

$$\tau = \frac{t}{H/U_0}, p^* = \frac{p - p_\infty}{\sigma U_0 H B^2} \quad (27)$$

$$Re = \frac{\rho U_0 H}{\mu}, N = \frac{(Ha)^2}{Re} \quad (28)$$

$$\theta = \frac{T - T_0}{T_w - T_0} \quad (29)$$

$$Pr = \frac{v}{\alpha}, E = \frac{\alpha_1}{\rho H^2} \quad (30)$$

$$Gr = \frac{g\beta H^3 (T_w - T_0)}{v^2} \quad (31)$$

where Re is Reynolds Number, Gr is Grashof Number, Pr is Prandtl Number, N is magnetic parameter, $Ha (\equiv BH\sqrt{\sigma/\mu})$ is Hartmann Number, H is characteristic length, E is the elasticity coefficient, U_0 is the fluid inlet average speed will be (26) ~ (31) style dimensionless parameters into (21), (22), (23) and (24) type, we get the governing equations dimensionless as:

Continuity equation:

$$\frac{\partial U}{\partial X} + \frac{\partial V}{\partial Y} = 0 \quad (32)$$

Momentum equation:

$$\begin{aligned} \frac{\partial U}{\partial \tau} + U \frac{\partial U}{\partial X} + V \frac{\partial U}{\partial Y} &= \\ -\frac{\partial p^*}{\partial X} + \frac{1}{Re} \left(\frac{\partial^2 U}{\partial X^2} + \frac{\partial^2 U}{\partial Y^2} \right) & \\ + E \left[\left(\frac{\partial^3 U}{\partial X^2 \partial \tau} + \frac{\partial^3 U}{\partial Y^2 \partial \tau} \right) + 2 \frac{\partial^2}{\partial X^2} \left(U \frac{\partial U}{\partial X} + V \frac{\partial U}{\partial Y} \right) \right. & \quad (33) \\ + 4 \left(\frac{\partial U}{\partial X} \frac{\partial^2 U}{\partial X^2} + \frac{\partial V}{\partial X} \frac{\partial^2 V}{\partial X^2} \right) + \frac{\partial^2}{\partial X \partial Y} \left(U \frac{\partial V}{\partial X} + V \frac{\partial V}{\partial Y} \right) & \\ + \frac{\partial^2}{\partial Y^2} \left(U \frac{\partial U}{\partial X} + V \frac{\partial U}{\partial Y} \right) + 2 \frac{\partial}{\partial Y} \left(\frac{\partial U}{\partial X} \frac{\partial U}{\partial Y} + \frac{\partial V}{\partial X} \frac{\partial V}{\partial Y} \right) & \\ + \frac{Gr}{Re^2} \theta \sin\phi - Nb(bU - aV) & \end{aligned}$$

$$\begin{aligned} \frac{\partial V}{\partial \tau} + U \frac{\partial V}{\partial X} + V \frac{\partial V}{\partial Y} &= \\ -\frac{\partial p^*}{\partial Y} + \frac{1}{Re} \left(\frac{\partial^2 V}{\partial X^2} + \frac{\partial^2 V}{\partial Y^2} \right) & \\ + E \left[\left(\frac{\partial^3 V}{\partial X^2 \partial \tau} + \frac{\partial^3 V}{\partial Y^2 \partial \tau} \right) + 2 \frac{\partial^2}{\partial Y^2} \left(U \frac{\partial V}{\partial X} + V \frac{\partial V}{\partial Y} \right) \right. & \quad (34) \\ + 4 \left(\frac{\partial U}{\partial Y} \frac{\partial^2 U}{\partial Y^2} + \frac{\partial V}{\partial Y} \frac{\partial^2 V}{\partial Y^2} \right) + \frac{\partial^2}{\partial X \partial Y} \left(U \frac{\partial U}{\partial X} + V \frac{\partial U}{\partial Y} \right) & \\ + \frac{\partial^2}{\partial X^2} \left(U \frac{\partial V}{\partial X} + V \frac{\partial V}{\partial Y} \right) + 2 \frac{\partial}{\partial X} \left(\frac{\partial U}{\partial X} \frac{\partial U}{\partial Y} + \frac{\partial V}{\partial X} \frac{\partial V}{\partial Y} \right) & \\ + \frac{Gr}{Re^2} \cos\phi - Na(aV - bU) & \end{aligned}$$

Energy equation:

$$\frac{\partial \theta}{\partial \tau} + U \frac{\partial \theta}{\partial X} + V \frac{\partial \theta}{\partial Y} = \frac{1}{Re Pr} \left(\frac{\partial^2 \theta}{\partial X^2} + \frac{\partial^2 \theta}{\partial Y^2} \right) \quad (35)$$

where E is elastic modulus, high-risk of the item shall be included in the governing equations of elastic terms. $1/Re$

traveled on the item shall be included in the governing equations of Adhesion term. If the elastic coefficient $E = 0$, $N = 0$, the governing equation can be simplified to our well-known two-dimensional governing equations for Newtonian fluids.

Solving two-dimensional, incompressible flow field, the use of flow lines vorticity equation to replace the speed and pressure equation of its advantages are:

- 1) Four governing equations will be reduced to three, automatically satisfy the continuity equation.
- 2) Demand pressure term to avoid the border when the pressure encountered difficulties in setting the value.

In the conversion process variables, the use of vorticity and stream function replaces the governing equations in the velocity and pressure variables, and the vorticity vector is defined as:

$$\bar{\omega} = \nabla \times \mathbf{V} \quad (36)$$

The pure volume is expressed as:

$$\omega = |\bar{\omega}| = |\nabla \times \mathbf{V}| \quad (37)$$

In Cartesian coordinate can be written as:

$$\omega = \frac{\partial V}{\partial X} - \frac{\partial U}{\partial Y} \quad (38)$$

In the same coordinate system, the stream function ψ defined as:

$$\frac{\partial \psi}{\partial Y} = U \quad (39)$$

$$-\frac{\partial \psi}{\partial X} = V$$

Using these definitions as a new dependent variable and equation (34) on the X-type differential, and less equation (33) on the Y-type differential. Where equation (33) and equation (34) where the pressure of the two items, therefore the momentum equation is eliminated, which combined vorticity equation in the form of:

$$\begin{aligned} & \frac{\partial \omega}{\partial \tau} + \frac{\partial(U\omega)}{\partial X} + \frac{\partial(V\omega)}{\partial Y} \\ &= \frac{1}{Re} \left(\frac{\partial^2 \omega}{\partial X^2} + \frac{\partial^2 \omega}{\partial Y^2} \right) + E \left[\frac{\partial}{\partial \tau} \left(\frac{\partial^2 \omega}{\partial X^2} + \frac{\partial^2 \omega}{\partial Y^2} \right) \right. \\ &+ \frac{\partial^2}{\partial X^2} \left(U \frac{\partial \omega}{\partial X} + V \frac{\partial \omega}{\partial Y} \right) + \frac{\partial^2}{\partial Y^2} \left(U \frac{\partial \omega}{\partial X} + V \frac{\partial \omega}{\partial Y} \right) \\ &+ 4 \left(\frac{\partial^2 U}{\partial X \partial Y} \frac{\partial^2 U}{\partial Y^2} + \frac{\partial U}{\partial Y} \frac{\partial^3 U}{\partial X \partial Y^2} - \frac{\partial^2 V}{\partial X \partial Y} \frac{\partial^2 V}{\partial X^2} - \frac{\partial V}{\partial X} \frac{\partial^3 V}{\partial X^2 \partial Y} \right) \\ &+ 2 \left(\frac{\partial V}{\partial Y} \frac{\partial^3 V}{\partial X^3} - \frac{\partial U}{\partial X} \frac{\partial^3 U}{\partial Y^3} - \omega \frac{\partial^3 U}{\partial X^3} - \omega \frac{\partial^3 V}{\partial Y^3} \right) \\ &+ \frac{Gr}{Re^2} \left(\frac{\partial \theta}{\partial X} \cos \phi - \frac{\partial \theta}{\partial Y} \sin \phi \right) + N \left(a^2 \frac{\partial^2 \psi}{\partial X^2} + b^2 \frac{\partial^2 \psi}{\partial Y^2} \right) \quad (40) \end{aligned}$$

The U , V to equation (39) substitution of the form equation (40) to obtain ω and ψ available to the vorticity equation for the variables and the dimensionless temperature variable θ is the energy equation.

$$\begin{aligned} & \frac{\partial \omega}{\partial \tau} + \frac{\partial(U\omega)}{\partial X} + \frac{\partial(V\omega)}{\partial Y} \\ &= \frac{1}{Re} \left(\frac{\partial^2 \omega}{\partial X^2} + \frac{\partial^2 \omega}{\partial Y^2} \right) + E \left[\frac{\partial}{\partial \tau} \left(\frac{\partial^2 \omega}{\partial X^2} + \frac{\partial^2 \omega}{\partial Y^2} \right) \right. \\ &+ \left(\frac{\partial^3 \psi}{\partial X^2 \partial Y} \frac{\partial \omega}{\partial X} + \frac{\partial \psi}{\partial Y} \frac{\partial^3 \omega}{\partial X^3} - \frac{\partial^3 \omega}{\partial X^2 \partial Y} \frac{\partial \psi}{\partial X} - \frac{\partial \omega}{\partial Y} \frac{\partial^3 \psi}{\partial X^3} \right. \\ &+ \left(\frac{\partial^3 \psi}{\partial Y^3} \frac{\partial \omega}{\partial X} + \frac{\partial \psi}{\partial Y} \frac{\partial^3 \omega}{\partial Y^3} - \frac{\partial^3 \omega}{\partial Y^3} \frac{\partial \psi}{\partial X} - \frac{\partial \omega}{\partial Y} \frac{\partial^3 \psi}{\partial Y^2 \partial X} \right) \\ &+ 4 \left(\frac{\partial^3 \psi}{\partial X \partial Y^2} \frac{\partial^3 \psi}{\partial Y^3} + \frac{\partial^2 \psi}{\partial Y^2} \frac{\partial^4 \psi}{\partial X \partial Y^3} - \frac{\partial^3 \psi}{\partial X^2 \partial Y} \frac{\partial^3 \psi}{\partial X^3} - \frac{\partial^2 \psi}{\partial X^2} \frac{\partial^4 \psi}{\partial X^3 \partial Y} \right) \\ &+ 2 \left(\frac{\partial^2 \psi}{\partial X \partial Y} \frac{\partial^4 \psi}{\partial X^4} - \frac{\partial^2 \psi}{\partial X \partial Y} \frac{\partial^4 \psi}{\partial Y^4} - \omega \frac{\partial^4 \psi}{\partial X^3 \partial Y} + \omega \frac{\partial^4 \psi}{\partial X \partial Y^3} \right) \\ &+ \frac{Gr}{Re^2} \left(\frac{\partial \theta}{\partial X} \cos \phi - \frac{\partial \theta}{\partial Y} \sin \phi \right) + N \left(a^2 \frac{\partial^2 \psi}{\partial X^2} + b^2 \frac{\partial^2 \psi}{\partial Y^2} \right) \quad (41) \end{aligned}$$

$$\frac{\partial \theta}{\partial \tau} + U \frac{\partial \theta}{\partial X} + V \frac{\partial \theta}{\partial Y} = \frac{1}{RePr} \left(\frac{\partial^2 \theta}{\partial X^2} + \frac{\partial^2 \theta}{\partial Y^2} \right) \quad (42)$$

At the same time then equation (39) substitution equation (38), we have ω and ψ obtained for the other variables in the equation, as follows:

$$\frac{\partial^2 \psi}{\partial X^2} + \frac{\partial^2 \psi}{\partial Y^2} = -\omega \quad (43)$$

This'd elliptical partial differential equations known as the Poisson equation. In the process of solving the flow field, the solutions of the vorticity field by equation (41), then this vorticity into equation (43) where calculated stream function. And anti-reflux stream function on behalf of the definition of equation (39), we can obtain the velocity field. Velocity vector then substituted into the energy equation (42), we obtain the temperature field. And determine whether it reached convergence conditions, if the conditions are not, then go back and drive solutions of the vorticity transport equation.

C. Initial and Boundary Conditions

The governing equations of this paper is dimensionless, its X, Y coordinates in terms of equation of elliptic type is still, so each physical quantity ψ , ω , θ , in the calculation of each boundary must be Set the boundary values, these values were set at the entrance, down, step plate and exit. Flow field in the start of this article remain static, the interior points of the initial value are zero, the boundary conditions given as follows:

- 1) Upstream entrance:

State flow field is assumed to be the fully developed entrance flow, under the assumption that the flat plate and the value of difference between the stream line one. Durst and Pereira [3] used TEACH software package for transient flow analysis, and the study used fully development uniform flow such as different inlet conditions, the effect of the flow field. Although their conclusion is as fully developed flow, transient flow entrance conditions, similar to artificial are suspected. But the numerical results and experimental measurement results compared to the flow field affect only the start of a number of intervals, and the results differ little. So consider that as a fully developed flow, the inlet conditions of transient flow field are still

reasonable.

$$\text{inlet velocity: } U = U(Y) = -48(Y - 0.5)^2 + 24(Y - 0.5)$$

$$\text{vertical velocity: } V = \frac{\partial V}{\partial X} = \frac{\partial V}{\partial Y} = \frac{\partial U}{\partial X} = 0$$

inlet stream function:

$$\psi = \int_{0.5}^1 U dY = -16(Y - 0.5)^3 + 12(Y - 0.5)^2$$

inlet temperature: $\theta = 0$

2) Solid boundary:

on the board: The no slip condition:

$$\text{velocity: } U = V = 0$$

$$\text{stream function: } \psi = 1$$

$$\text{adiabatic heat transfer boundary conditions: } \partial\theta/\partial Y = 0$$

down the board and ladder surface: The no slip condition:

$$\text{velocity: } U = V = 0$$

$$\text{stream function: } \psi = 0$$

constant temperature in heat transfer boundary conditions:

3) Downstream outlet: The Neumann boundary conditions

$$\text{velocity: } \partial U / \partial X = \partial V / \partial X = 0$$

$$\text{stream function: } \partial \psi / \partial X = 0$$

$$\text{vorticity function: } \partial \omega / \partial X = 0$$

$$\text{temperature function: } \partial \theta / \partial X = 0$$

4) Magnetic field boundary conditions: the magnetic field is constant.

II. PROBLEM SOLUTION

This paper analyzes the application of numerical methods, mainly finite difference method to calculate the grid for the uniform grid. As the grid used for the uniform grid, the grid points in the choice of when to pay special attention, grid points are too sparse, if taken, will affect the accuracy of the results, if taken too close, then the computing time and the dramatic increase in computer memory space will be. In order to select the grid spacing to resolve the problem by numerical analysis of experimental results, this paper choose $385 \times 33, 544 \times 33, 673 \times 33$ grid points to compare three different calculations, and finally with 673×33 grid points to simulate analysis.

The reference is raised Yoo [26] visco-elastic fluid grid spacing of the proposal. As taking into account the results and accuracy, and to avoid visco-elastic fluid composition of the existence of highly nonlinear equations, which will consume a lot of computing time and computer memory space deficiencies. The proposed lattice spacing equal to $\Delta X = \Delta Y = 1/16$, will be able to meet both needs. In order to further solve the more accurate results, in conjunction with the reality of computer equipment capacity, with grid spacing equal to $\Delta X = \Delta Y = 1/32$. The X direction of the choice of the length of the report from the literature, there are two basic ways Chein [5] : 1 six times for the selection of step length, the other is twelve times.

Because the treatment of governing equations for the highly nonlinear partial differential equations. So, the numerical procedures must be linear, and the layout of each time through

constant iteration calculation in order to achieve convergence of results. Vorticity equation used in the numerical iterative method is the line-Gauss-Seidel method and the interaction with the scanning application. As the equation is nonlinear, into a linear processing in the iterative calculation may cause numerical divergence, the vorticity function at the same time and energy in the equation by adding under-relaxation, in the stream function by adding over-relaxation, in order to avoid numerical divergence occurs. Due to the vorticity equation, flow line equation and the energy equation by adding relaxation terms, numerical calculations can be made with three adjustable relaxation coefficients, an increase of numerical superiority. We can adjust the three relaxation coefficients, in order to avoid numerical divergence and to accelerate the numerical convergence.

Here, we introduce relaxation method principles and techniques, and explain the Gauss – Seidel method through relaxation and well-combined and interactive continuous scanning applications. The Gauss-Seidel method such numerical methods can be further divided into point iteration method and the block iterative method. In point iterative process, the main application is the same polynomial unknown variables at each grid point to consider, then scanning iteration to the next row or column.

Gauss-Seidel iteration, if used in the elliptic partial differential equations called to Liebmann iteration. Formula for dealing with large systems, this method is more efficient numerical procedure. This method is very simple, but only in certain conditions in order to obtain convergence results, in general can be diagonally dominant matrix of coefficients to explore. We use Laplace equation to discuss the line Gauss – Seidel method suitably.

For many of the flows, the boundary treatment is often the most difficult, the border is also the numerical instability caused by divergence of the main factors, especially in the geometric shape of the corner. The visco-elastic fluid constitutive equation because of its complicated than the Newtonian fluid, numerical target because the border has made a series of processing, are introduced in each border several different approaches, to identify the most appropriate boundary equations.

III. RESULTS AND DISCUSSION

In this paper, it is using the numerical analysis of visco-elastic fluid flow in the backward facing step phenomena. The article compared the results of elasticity but set to 0, Reynolds Number 50, Richardson Number 1, and Prandtl Number 0.7 flow field, and Hsu [20] to verify the transient Nusselt coefficient comparison, from Figure 2, Figure 3 shows a consistent trend of the two plans, it has considerable accuracy.

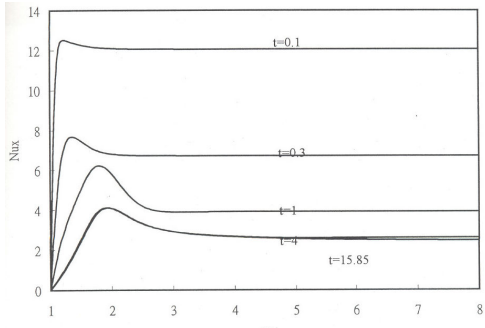


Fig. 2 the Nesslt coefficient distribution by Hsu[20]

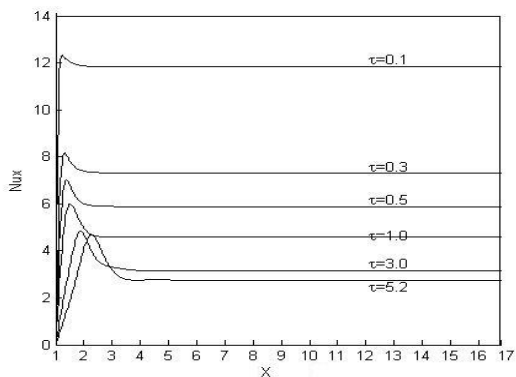


Fig. 3 the Nesslt coefficient distribution with this article.

This flow fields for the forced convection and natural convection coupled mixed convection. Therefore we define the Richardson Number of $Ri = Gr/Re^2$, to indicate the buoyancy effect, and to further explore the relatively strong natural convection. Richardson Number in the calculation were 12 and 16, select these two parameters is due to Richardson Number a few less than 12 cases, in addition to the primary recirculation zone reattachment length increases, there is no other special situation, the number, but when Richardson Number greater than 12, with the increase in Reynolds Number will result in separation of recirculation zone, it is equal to the Richardson Number of selected 12 and 16 to explore.

As for the choice of Reynolds Number were set to 50 and 75, because the visco-elastic fluid, the Reynolds Number over 100 will be developed into a turbulent flow, not only easily lead to numerical divergence, and the assumption of laminar flow and does not meet, so I chose to use Reynolds Number equal to 50 and 75. Elasticity value of 0.0005 and 0.001 selected, Prandtl Number = 0.7, flow angle is fixed 0° . Then the length of the ladder 15 times the flow field is set to high, followed by flow field, vorticity field, velocity field, temperature field of development, and re-attachment length to be discussed.

When the fluid flows through a convex angle, because of sharp points of the relationship between the radius of curvature and pressure will produce separation. In order to calculate the location of separation point, this article uses Roache and Muller [28] method does not set in the convex corner separation point, the decision by the results.

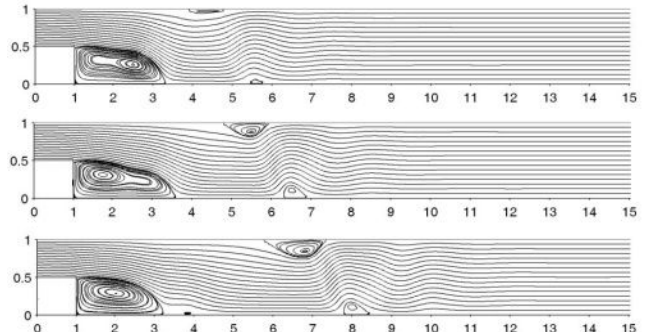
Fig. 4 $Ri=16$, $Re=50$, $E=0.0005$, $t=15$, $N=1.5, 1, 0.5$

Figure 4 Richardson Number 16, Reynolds Number 50 and elastic coefficient 0.0005 to discuss and compare. We can see that the upper and lower flat area will appear the phenomenon of sub-return, but with the development of the steady-state flow field and disappear.

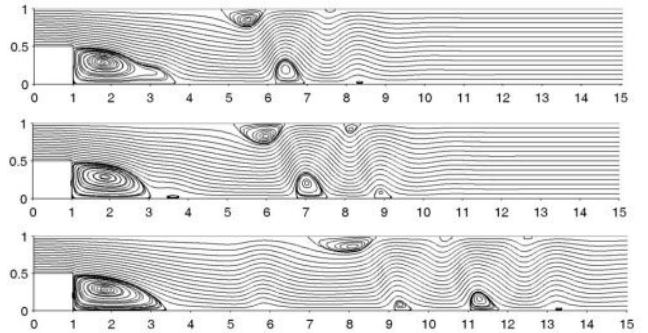
Fig. 5 $Ri=16$, $Re=50$, $E=0.001$, $t=15$, $N=1.5, 1, 0.5$

Figure 5 Richardson Number 16, Reynolds Number 50, and coefficient of elasticity 0.001 compared to the upper and lower plate will be four times the recirculation transient coexistence. The reason may be caused by a high coefficient of elasticity greater cohesion between fluid particles, leading to dissipation and time-consuming second recirculation region is longer, resulting in lower reaches of the middle part of the primary recirculation zone occurred several times recirculation transient coexistence, up and down the four flat a second recirculation zone exist, but with the steady flow of development, eventually dissipated. When the flow reached steady state, the flow line is not the whole show flow situation, but somewhat similar to the fluctuating reach convergence.

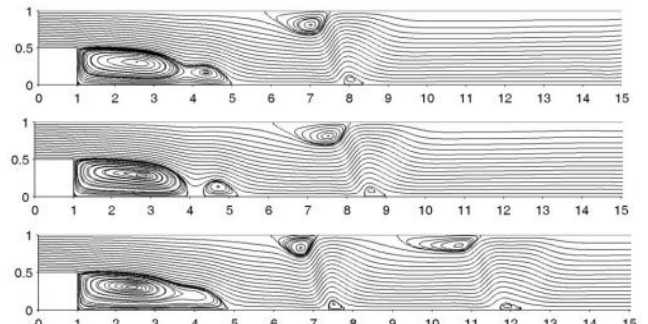
Fig. 6 $Ri=16$, $Re=75$, $E=0.0005$, $t=15$, $N=1.5, 1, 0.5$

Figure 6 and then the Richardson Number of logical investigation of 16, when the elastic coefficient of 0.0005, the Reynolds Number increased to 75, due to higher flow rate, in order to stimulate the primary recirculation zone extends continuously downstream, with little cohesion between fluid particles and ultimately isolated from the primary recirculation phenomenon of second recirculation zone, and the isolated area produced plays back gradually move downstream, and finally dissipated. The dissipation is stability in the flow field before the separation occurs four times.

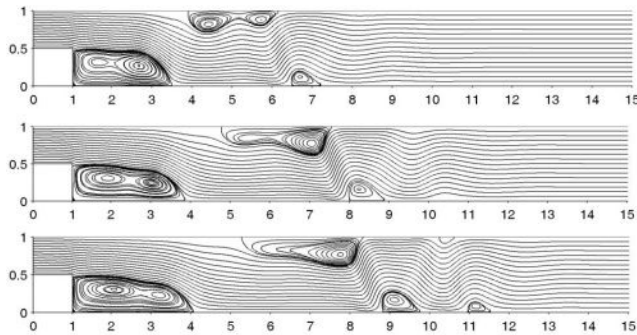


Fig. 7 $Ri=16$, $Re=75$, $E=0.001$, $t=15$, $N=1.5,1,0.5$

Figure 7 for the Richardson Number 16, Reynolds Number 75, when the elastic coefficient of 0.001 cases of development, due to the higher elastic effect, causing the primary recirculation zone separating the phenomenon of second recirculation zone occurs only once, is now considered as times the length of the longest reflux zone.

From this high Richardson Number few indeed injured by the primary recirculation zone becomes larger, and then attached to increase the length of the effect of the magnetic field parameters were restrained for Eddy. Apart from the magnetic field strength generated can prevent the boundary layer separation, the boundary layer when the magnetic field strength obtained in large enough, the flow lines become narrower and with a little acceleration to be effective, and the literature made by Hong [22] consistent results. But when the primary recirculation District, to a certain extent, because the fluid particles with each other less flexibility and flow faster, while the front driving the primary recirculation zone separation phenomenon began, but many times after the separation is no longer the primary recirculation zone separation and stabilization, and finally reaches a steady state. The effect may be reduced because of the heat transfer caused by lack of energy, so that is no longer isolated from the primary recirculation zone plays back area.

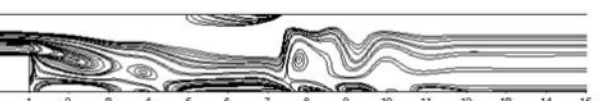
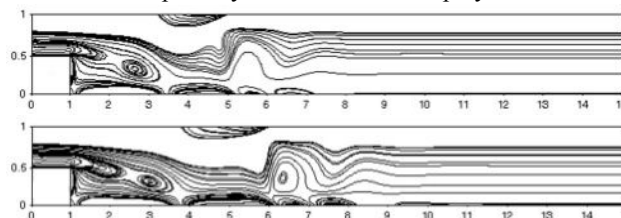


Fig. 8 $Ri=16$, $Re=50$, $E=0.0005$, $t=15$, $N=1.5,1,0.5$

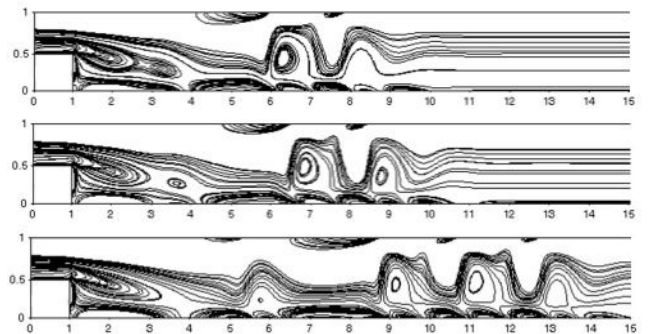


Fig. 9 $Ri=16$, $Re=50$, $E=0.001$, $t=15$, $N=1.5,1,0.5$

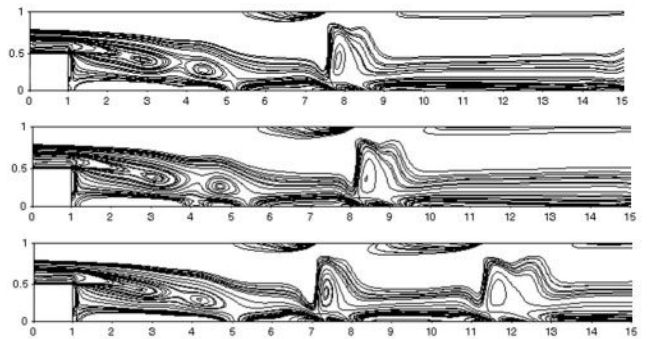


Fig. 10 $Ri=16$, $Re=75$, $E=0.0005$, $t=15$, $N=1.5,1,0.5$

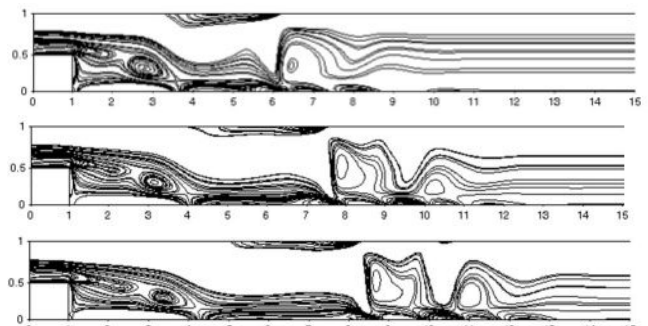


Fig. 11 $Ri=16$, $Re=75$, $E=0.001$, $t=15$, $N=1.5,1,0.5$

Figure 8, Figure 9, Figure 10, and Figure 11 for the vortex parameters such as Richard few different development situations. Can be seen from the diagram, that exist at the entrance of vorticity due to the entry for a given initial velocity distribution for the parabolic relationship, it is not zero. And downstream near the vorticity lines can be seen with dense concave wall occurs, and then increase with time, eddy diffusion approach will flow to the internal transfer, over a period of time, the entrance vortex lines become more parallel. Then we can see the point in the ladder convex, showing a high density of vortex lines that at this higher vorticity gradient. As the fluid flow around the convex corner vortex line slowly spread to the lower

step, then it is clear that the extension of the convex corner from under the tongue, etc. vorticity lines. Then this intensive vorticity lines such as the impact due to water flow down the stretch, slowly lower the density of its gathering, and finally reaches a steady state. And so the development of vorticity lines to follow the precedent of flow chart, you can see some of the region downstream flow will be streaming up and down the situation, but it will not happen times back area, probably because such vortex lines in the region is not enough intensive, so it cannot form a second recirculation zone.

When there are multiple co-exist for the second recirculation zone, you can see so many closed vorticity lines exist. Discuss the data obtained can be related to vorticity that, at a fixed Reynolds Number and the flexibility coefficient, Richard higher the magnetic field parameters of the more hours, the steady-state is under the plate the greater the maximum vorticity. That the effects of thermal convection sudden change in flow area will be on enhancing the role of the vorticity generated. At fixed Reynolds Number, Richard few parameters and magnetic field, the greater the elasticity coefficient will result in steady state under the plate is smaller vorticity extremism. From this, the elastic effect of sudden change in the flow field vorticity region will produce inhibition.

In this Figure, $\omega = 0$ is for the horizontal line of the junction, also re-attached to the primary recirculation zone length location. With Richardson Number and elastic coefficient increase, we can find some curve to negative after the local minimum and does not rise to a fixed value; the stability extends to the exit. This phenomenon may be caused by the high Richardson Number, the larger buoyancy effect, resulting in up and down oscillation of the vorticity present situation. However, only the upper and lower range of oscillation negative vorticity region as there has not been the case $\omega = 0$ over the horizon. Hsu [20] has said that eddy down to after the local minimum and then rose up over the $\omega = 0$ time horizon, is also positive vorticity, this indicated the existence of steady-state plays back area. However, this study did not occur in this phenomenon, we generated non-stationary time back area.

IV. CONCLUSION

In the thermal flow researches, the post-flow analysis to the backward facing step model can be regarded as a flow field. As the magnetic fluid viscoelastic constitutive equation is more complicated, so many studies are limited to analysis of the effect of boundary layer and the elastic effect, without further in depth. For this point, this article viscoelastic magnetic fluid used in the backward facing step with a mixed convection flow, and further enhance its natural convection and then to analyze the effect of flow fields.

They were along larger buoyancy effect with Richardson Number. Can be found downstream of the primary recirculation step multiple second recirculation zone appears transient coexistence, the four vortexes appeared on the upper and lower plate, and it was in symmetry. The primary recirculation zone because of the high buoyancy and thermal convection effect, so

isolated from the primary recirculation zone plays back area, and repeated four times each separate time, in the attachment are slightly extended length. Will then decrease due to heat convection and flatten, rather than isolated plays back area, this phenomenon is somewhat similar to Karman vortex of the oscillation phenomena.

Buoyant conditions in the larger flow field, and finally reaches the steady state of flow is not for the whole development of flows, but a little wave-like phenomenon, the primary recirculation zone and then attached to the longer length with the higher Richardson Number. Buoyancy effect increases, the isotherm by its effect, it is more behind the development of flow field, keep up the isotherms can be seen floating flat stretch. And the position of contact with the plate also was a bit upstream, so the greater the buoyancy effect on the temperature field is higher.

Have the same Richardson Number, Reynolds Number, and the elastic coefficient, the higher the magnetic field parameters of the main and second recirculation zone and then attached to the shorter length. Because the magnetic field parameters were restrained for the eddy current, magnetic field strength in addition to boundary layer separation can prevent the generation of foreign, when the magnetic field strength in the boundary layer was large enough, the flow lines become narrower and with a little acceleration effect.

REFERENCES

- [1] Honji H., "The Starting Flow Down a Step," *J.Fluid Mech.*, Vol.69, Part2, 1975, p.p.317-325.
- [2] Armaly B.F., Durst F., Pereira J.C.F. and Schonumy B., "Experimental and Theoretical Investigations of Backward Facing Step Flow," *J.Fluid Mech.*, Vol.127, 1983, pp.473 -496.
- [3] Durst F. and Pereira J.C.F., "Time-Dependent Laminar Backward Facing Step Flow in a Two-Dimensional Duct," *ASME J.of Fluid Engeering*, Vol.110, 1988, pp.289-296.
- [4] Sparrow E.M. and Chuck W., "PC Solution for Heat Transfer and Fluid Flow Downstream of an Abrupt Asymmetric Enlargement in Channel," *Numerical Heat Transfer*, Vol.12, 1987, pp.19-40.
- [5] Reiyu R.Chein, "Numerical Modelling of Unsteady Backward facing Step Flow," *J. of Chinese Institute of Engineers*, Vol.13, No.1, 1990, pp.69-82.
- [6] Johan M. and Leone J.R., "Open Boundary Condition Symposium Benchmark Solution : Stratified Flow Over a Backward Facing Step," *Int. J. Numerical Method in Fluids*, Vol.11, 1990, pp.969-984.
- [7] Lin J.T. , Armaly B.F. and Chen T.S., "Mixed Convection in Buoyancy-Assisting Vertical Backward Facing Step Flow," *Int. J. Heat and Mass Transfer*, 1990, pp.2121-2131.
- [8] Nobuyoshi Kawabata, Isao Ashino, Motoyoshi Tachibana and Katsushi Fujita, "Backward Facing Step Flow of Viscoelastic Fluids," Nippon KiKai Gakkai Ronbunshu B, Vol.55, n.518, 1989, pp.2977-2982.
- [9] Chan C.K., Zhang H.Q.,and Lau K.S., "Numerical simulation of gas-particle flows behind a backward facing step using an improved stochastic flow model," *Computational Mechanics*, Vol.39, 2001, pp.412-417.
- [10] Piccolo C., Arina R. and Cancelli C., "Fluid Exchange Between a Recirculation Region and the Perturbed External Flow," *Phys. Chem. Earth(B)*, Vol.26, NO.4, 2001, pp.269-273.
- [11] Abu-Hijleh B.A/K, "Heat transfer from a 2D backward facing step with isotropic porous floor segments," *International Journal of Heat and Mass Transfer*, Vol.43, 2000, pp.2727-2737.
- [12] Kim S.S. and Baek S.W., "Radiation affected compressible turbulent flow over a backward facing step," *Int. J. Heat and Mass Transfer*, Vol.39, NO.16,1996, pp.3325-3332.

- [13] Abu-Mulaweh H.I., Armaly B.F., Chen T.S., "Turbulent mixed convection flow over a backward-facing step," *International Journal of Heat and Mass Transfer*, Vol.44, 2001, pp.2661-2669.
- [14] Vest C.M. and Arpacı V.S., "Overstability of a Viscoelastic Fluid Layer Heated from Below," *J. Fluid Mech.*, Vol.36, 1969, pp.613-623.
- [15] Herbert D.M., "On the Stability of Viscoelastic Liquids in Heated Plane Couette Flow," *J. Fluid Mech.*, Vol.17, 1963, pp.353-359.
- [16] Hsu C.H. and Chieng J.S., "Mixed Convection of a Viscoelastic Fluid on a Horizontal Flat Plate," *The Fifteenth National Conference on Theoretical and Applied Mechanics*, Taiwan, R.O.C, 1991 pp.481-488.
- [17] Hsu C.H., Chen C.S. and Teng J.T., "Effect of Fluid Viscoelasticity on Wedge Flow with Injection or Suction," *The Chung Yuan Journal*, 1991, pp.74-85.
- [18] Hsu C.H. and Chou T.Y., "Unsteady flow of a second-grade fluid past a backward-facing step," *International Journal of Non-Linear Mechanics*, Vol.32, No.5, 1997, pp.947-960.
- [19] Hsu C.H., Chen Y.P., Chen B.C., "Transient mixed convection of a second-grade fluid past a backward-facing step," *International Journal of Non-Linear Mechanics*, Vol.34, Issue:5, 1999, pp.881-893
- [20] Kung K.Y., Hsu C.H., Chiang H.L., "Transient mixed convection flow of a second grade viscoelastic fluid past an inclined backward facing step," *International Journal of Non-Linear Mechanics*, Vol.39, Issue:7, 2004, pp.427-429.
- [21] Wang J. C., Liu Y. Z., "Laminar MHD mixed convection in vertical channel," *Electronic Theses and Dissertation System*, 2006.
- [22] Hong Z. J., Lin S. Y., "Numerical simulation of two-dimensional incompressible MHD flow," *Electronic Theses and Dissertation System*, 2003.
- [23] Weng H. C., Chen C. L., Chen C.K., "Non-Newtonian flow of dilute ferrofluids in a uniform magnetic field," *Physical Review E* 78, 2008
- [24] Rivlin R.S. and Erickson J.L., "Stress deformation relation for isotropic materials," *J. rat. Mech. Analysis* 4, 1995, pp.323-425.
- [25] Rajagopal K.R., Gupta A.S. and Wineman A.S., "On a Boundary Layer Theory for non-Newtonian fluids," *Lett Appl. Sci. Engng*, Vol.18, 1980, pp.875-883.
- [26] Song J.H. and Yoo J.Y., "Numerical Simulation of Viscoelastic Flow Through a Sudden Contraction Using a Type Dependent Difference Method," *J. Non-Newt. Fluid Mech.*, Vol.24, 1987, pp.221-243.
- [27] Rajagopal K. R. and Fosdick R. L., "Uniqueness and Drag for Fluids of Second Grade in Steady Motion," *J. of Non-Linear Mechanics*, Vol.13, 1978, pp.131-137.
- [28] Roache R.J. and Mueller T.J., "Numerical Solutions of Laminar Separated Flows," *AIAA J.*, Vol.8, 1970, pp.520-538.

Hsu is a full professor in the Mechanical Engineering Department. Expertise include engineering mathematics, thermodynamics, fluid mechanics, heat transfer, convective heat transfer, computational fluid mechanics, experimental methods of thermo-fluid mechanics and engineering acoustics, and research is in the analysis, visualization and measurement of fundamental flow and thermal fields of Newtonian fluids, Non-Newtonian fluids, viscoelastic fluids, and interactions between different fluids. His research topics include the visualization and measurement of a turbulent water jet in a water tunnel. Recently, he is interested in the visualization and analysis of a long bubble driven flows in a circular tube, thermal properties measurement and heat transfer analysis of porous ceramic heat spreaders and heat transfer performance of high power LED arrays.

Kung is a full professor in the Mechanical Engineering Department. Expertise include engineering mathematics, thermodynamics, fluid mechanics, heat transfer, and research is in the analysis, visualization and measurement of fundamental flow and thermal fields of Newtonian fluids. Recently, he is interested in analytical heat transfer analysis of fins and heat transfer performance of high power LED arrays.

Hu is a Ph.D. student in the Mechanical Engineering Department. Expertise include engineering mathematics, thermodynamics, fluid mechanics, heat transfer, convective heat transfer, computational fluid mechanics, experimental methods of thermo-fluid mechanics and engineering acoustics.